CHINESE OPTICS LETTERS

Vol. 21, No. 12 | December 2023

Light field information transmission through scattering media with high fidelity

Jianwei Ye (叶建伟)[1], Tuqiang Pan (潘土强)[1], Kanpei Zheng (郑龛培)[2], Zhichao Luo (罗智超)[3], Yi Xu (徐 毅)[1*], Songnian Fu (付松年)[1], Yuncai Wang (王云才)[1], and Yuwen Qin (秦玉文)[1,4**]

[1] Guangdong Provincial Key Laboratory of Information Photonics Technology, Institute of Advanced Photonics Technology, School of Information Engineering, Guangdong University of Technology, Guangzhou 510006, China

[2] Department of Electronic Engineering, College of Information Science and Technology, Jinan University, Guangzhou 510632, China

[3] Guangdong Provincial Key Laboratory of Nanophotonic Functional Materials and Devices and Guangzhou Key Laboratory for Special Fiber Photonic Devices and Applications, South China Normal University, Guangzhou 510006, China

[4] Synergy Innovation Institute of GDUT, Heyuan 517000, China

*Corresponding author: yixu@gdut.edu.cn

**Corresponding author: qinyw@gdut.edu.cn

Received April 17, 2023 | Accepted July 14, 2023 | Posted Online November 30, 2023

Realizing high-fidelity optical information transmission through a scattering medium is of vital importance in both science and applications, such as short-range fiber communication and optical encryption. Theoretically, an input wavefront can be reconstructed by inverting the transmission matrix of the scattering medium. However, this deterministic method for retrieving light field information encoded in the wavefront has not yet been experimentally demonstrated. Herein, we demonstrate light field information transmission through different scattering media with near-unity fidelity. Multi-dimensional optical information can be delivered through either a multimode fiber or a ground glass without relying on any averaging or approximation, where their Pearson correlation coefficients can be up to 99%.

Keywords: light field information transmission; transmission matrix.
DOI: 10.3788/COL202321.121101

1. Introduction

Propagation of light in a scattering medium suffers from multiple scattering in a counter-intuitive way[1]. During the propagation in strongly scattering media, both the amplitude and phase information encoded in the wavefront of the incident light are very fragile, resulting in the seemly chaotic speckle output[2,3]. Although light propagation in a linear and a time-invariant dielectric medium is a deterministic process, the multiple scattering nature of such a medium inevitably imposes a great challenge to precisely retrieving the encoded light field information. Leveraging the unprecedented capabilities of wavefront shaping, seeing through an opaque medium becomes a reality[4,5]. In particular, the unique combination of wavefront shaping and scattering media resembles a powerful tool to manipulate multiple optical scattering[2,6], facilitating versatile functionalities in optical focusing[7–9], imaging[10–19], 3D holography[20–23] and fiber laser[24].

As a typical multiple input multiple output (MIMO) system, optical multiplexing of data transmission through a scattering medium enables promising applications in optical communications[25–27]. According to the transmission matrix (TM) theory, multiple input multiple output of light in a scattering medium can be modeled using a linear relationship,

$$\dot{E}_{\text{out}} = T\dot{E}_{\text{in}}, \tag{1}$$

where T is the TM (an $M \times N$ matrix), and $\dot{E}_{\text{in}}$ (an $N \times 1$ vector) and $\dot{E}_{\text{out}}$ (an $M \times 1$ vector) are the input and output complex amplitudes of light field, respectively. As long as the TM is accurately calibrated, the information encoded in the input wavefront can be precisely retrieved by using $\dot{E}_{\text{in}} = T^{-1}\dot{E}_{\text{out}}$, where T^{-1} is the inversion or pseudo-inversion of the measured TM for the scattering medium. However, various types of experimental noises impose a practical limit that makes both the TM and the output amplitude and phase of light field difficult to perfectly measure[28], and the inverse TM (ITM) for recovering the encoded wavefront is deemed to be impracticable[10,13,25,26,29]. As a result, realizing perfect retrieval of the input light field information through a scattering medium using the ITM remains a promising but unattainable theoretical prospect[4].

To date, sophisticated methods, including TM with a mean square optimized operator (MSO)[10], polarization TM with

© 2023 Chinese Optics Letters

an MSO[29], and speckle correlation scattering matrix (SSM)[13,25,26], have been proposed for regaining the encoded information instead using the ITM. However, all these methods rely strictly on either statistics[10,29] or theoretical approximation[13,25,26], which essentially limits the attainable fidelity. Furthermore, the state-of-the-art deep learning method also cannot perfectly tackle this challenge[30–33] where the achieved fidelity is still limited. In this Letter, we experimentally demonstrate the multi-dimensional light field information transmission through scattering media with near-unity fidelity.

2. Experiments and Methods

The experimental setup for calibrating the TM of a scattering medium is shown in Fig. 1, where the scattering medium can be either a 1-m multimode fiber (MMF, diameter $\phi = 400\,\mu$m, numerical aperture NA = 0.22, Newport) or a ground glass (DG10-600, Thorlabs). A continuous-wave (CW) laser (wavelength $\lambda = 532$ nm, MSL-S-532-50 mW CH80136, CNI) with a maximum power of 50 mW is used. A polarizer produces an incident laser beam with horizontal polarization for a phase-only spatial light modulator (SLM, PLUTO-NIR, Holoeye). An objective lens (Obj_1) and a lens (L_1) form a spatial filtering and collimating system to expand the laser source. An amplitude and phase-encoded input object $\dot{E}_{in}$ is generated at the proximal end of the scattering medium by the SLM. The amplitude and phase-encoded beam is coupled into the scattering medium using an objective lens (Obj_2), and the scattered light is collected by another objective lens (Obj_3) at the output of the scattering medium. Finally, the speckle is recorded by a complementary metal oxide semiconductor (CMOS) camera (MER-231-41U3C-L, Daheng Imaging) whose resolution and pixel size are 1920 × 1200 and 5.86 μm, respectively.

In general, the experimental noise can be reduced by using the MSO-based method instead of $\dot{E}_{in} = T^{-1}\dot{E}_{out}$ [10],

$$E_{in} = |(T^* T + \sigma U)^{-1} T^* (\dot{E}^2_{out} - \dot{E}^1_{out})|, \tag{2}$$

where E_{in} is a virtual amplitude image, σ is the experimental noise factor to be optimized, U is the identity matrix, and * represents the transpose conjugate of a matrix. The result of Eq. (2) is equivalent to the result of $|T^{-1}\dot{E}_{out}|$ when σ is set to 0, and $\dot{E}^2_{out} - \dot{E}^1_{out}$ is replaced by the complex light field $\dot{E}_{out}$ without the ensemble average. Therefore, it pinpoints that the precise measurement of the TM (T) and the output light field ($\dot{E}_{out}$) is the cornerstone for realizing high-fidelity data transmission using ITM.

The TM of the scattering medium is experimentally calibrated by modifying the full-field self-interference and four-step phase-shifting method[28,34].The Hadamard basis is used as the input basis. A blazed grating is introduced to achieve efficient phase modulation in the first-order diffraction light, which is crucial for the high-precision TM calibration and output light field measurement. Substantially different from previous methods[10,29], a true amplitude and phase-encoded object is created by a phase-only SLM using a double-phase method[35,36], enabling the multiplexing of independent light field information through the scattering medium. The spatial distribution of the two-dimensional light field can be expressed as $T(x,y) = A(x,y)e^{i\varphi(x,y)}$, where $A(x,y)$ is the targeted amplitude, and $\varphi(x,y)$ is the targeted phase. Two-dimensional complex field $T(x,y)$ can be decomposed into the sum of two phase functions, $P_1(x,y) = \varphi(x,y) + \arccos[A(x,y)/A_{max}]$ and $P_2(x,y) = \varphi(x,y) - \arccos[A(x,y)/A_{max}]$. When $A_{max} = 2$ and $T(x,y) = e^{iP_1(x,y)} + e^{iP_2(x,y)}$, the target optical field can then be generated by using the phase-only SLM. At the same time, the amplitude

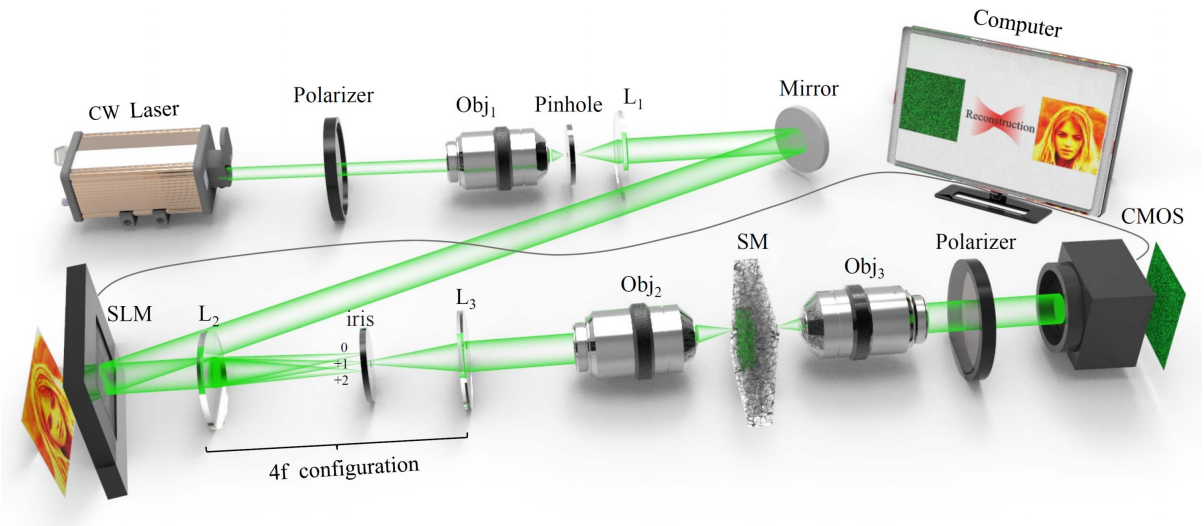

Fig. 1. Schematic and optical setup for realizing light field information transmission. "Obj" denotes microscopic objective (Obj_1, 20×, NA = 0.4; Obj_2 and Obj_3, 10×, NA = 0.25). L, lens (L_1 and L_2, focal length $f = 150$ mm; L_3, $f = 100$ mm). SM, a scattering medium that can be either an MMF or a ground glass. The iris is used for selecting the +1st order diffraction light for efficient phase modulation.

and phase information of the output light field $\dot{E}_{\text{out}}$ are acquired by generalizing the full-field self-interference and four-step phase-shifting method[28,34], which substantially improves the stability of the experimental setup. The $\dot{E}_{\text{out}}$ can be accurately obtained by

$$\dot{E}_{\text{out}} = \frac{(I^0 - I^\pi) + i(I^{3\pi/2} - I^{\pi/2})}{4\bar{R}}, \tag{3}$$

where R is the reference light field at the output of the scattering medium, " − " above R indicates complex conjugate, and I is the intensity recorded by the CMOS camera. The superscript of I denotes the corresponding phase shift. The influence of the reference field can be removed during $T^{-1}\dot{E}_{\text{out}}$ because of coaxial self-interference.

3. Results and Discussion

In order to verify the effectiveness of this method, we experimentally perform the data transmission mediated by the phase-encoded wavefront through an MMF first, as shown in Fig. 2(a). This figure shows that the quality of the reconstructed orbital angular momentum (OAM) holograms (256-level grayscale) with different topological charges ($l = 2$–7) by the ITM method is excellent, where the Pearson correlation coefficient (PCC; see Section 1 of the Supplementary Material) with near-unity fidelity (0.99) can be achieved. The retrieved results using the state-of-the-art MSO-based method[10] under the same experimental conditions are shown in Fig. 2(b). The reconstructed fidelity evaluated by structural similarity index measure (SSIM; see Section 1 of the Supplementary Material) of our method is much larger than that of the MSO-based method when no ensemble average is applied (1 realization and σ is optimized). Although the retrieved results using the MSO-based method can be improved by applying the ensemble average (50 realizations and σ is optimized), the achieved fidelity is still far from unity.

At the same time, the ratio γ between the output and input channel numbers also plays an important role in increasing the retrieving fidelity. Figure 2(c) shows that increasing γ will also improve the fidelity, where the influence of experimental noise on information retrieval is substantially reduced (see Section 2 of the Supplementary Material). According to the random matrix theory[37,38], the minimum normalized singular value of the TM is denoted by $\lambda_\gamma^{\text{Min}} = 1 - \sqrt{1/\gamma}$. The value of $\lambda_\gamma^{\text{Min}}$ increases together with the increasing of γ (see Fig. S1 of the Supplementary Material), and the contribution of a channel to the total energy transfer is proportional to the magnitude of the singular value[39]. This means that more speckle information is recorded by the camera at the output of the scattering medium

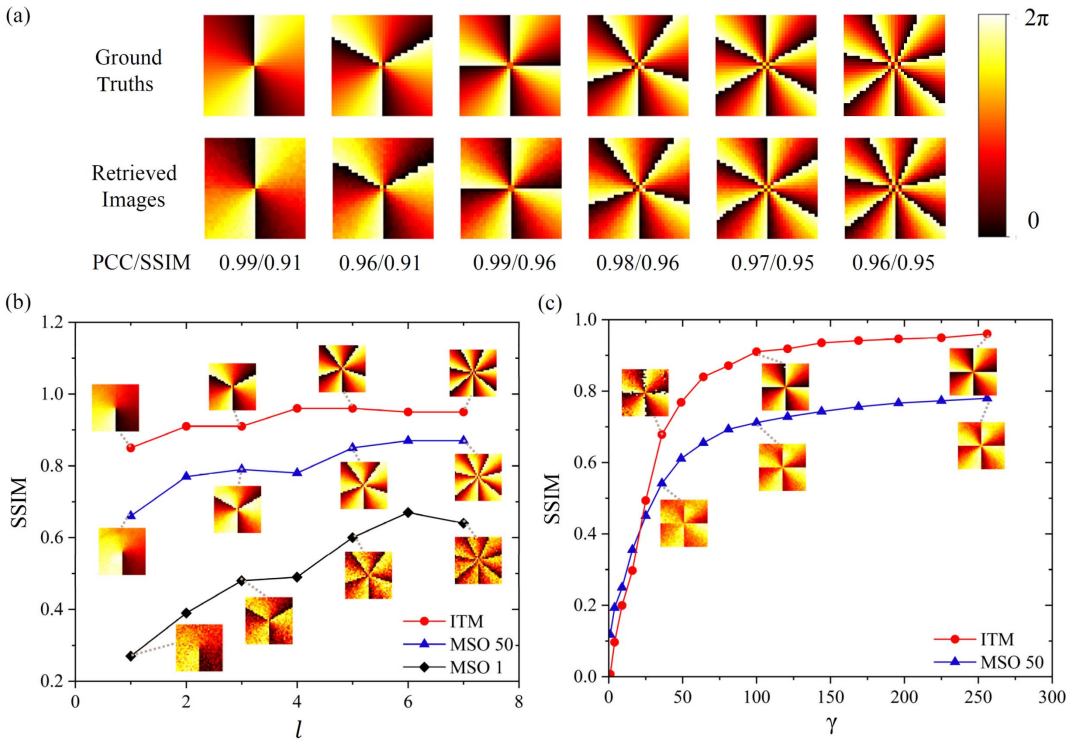

Fig. 2. Experimental phase retrieval results through an MMF based on the ITM method and the state-of-the-art MSO-based method. (a) Reconstruction of the 256-level grayscale OAM phase holograms with different topological values l ($l = 2$–7). The resolution of all holograms is 32×32. The corresponding PCC and SSIM for evaluating retrieved fidelity are also provided at the bottom of these figures. (b) Comparison of retrieval fidelity between the methods of ITM and MSO. Here, $M = 512 \times 512$ and $N = 32 \times 32$. (c) Dependence of the retrieval fidelity on the ratio (γ) between the output and input channel numbers for the ITM and MSO-based (50 realizations) methods. Typical retrieved results with different topological charges are shown in the insets of (b) and (c).

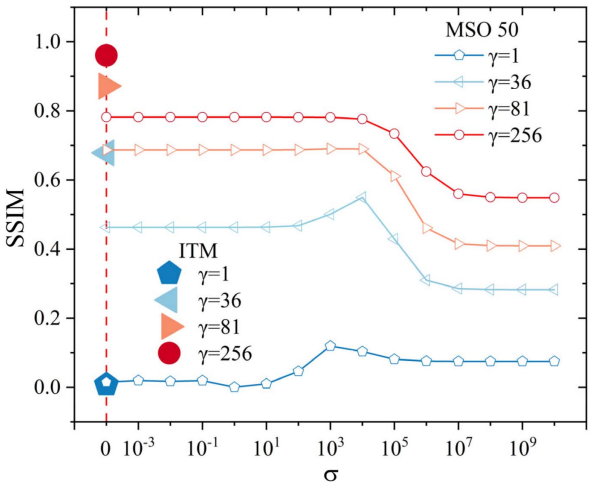

Fig. 3. SSIM of the retrieved OAM holograms ($l = 4$) as a function of the experimental noise factor σ. The results using the ITM method and the MSO-based method (50 averages) for different γ are shown in solid and open symbols, respectively.

for a larger γ, which results in more available spatial transmission channels to be selected, and more energy can be transmitted through the scattering medium.

As quantitatively shown in Fig. 3, the ITM method enables the near-unity fidelity of the data transmission (solid circle) compared with the MSO-based method (open circles and $\gamma = 256$, averaging over 50 realizations) under the same experimental conditions. It should be emphasized that the time consumption of the MSO-based method is 100 times of our case. When the experimental noise dominates the energy transfer channel (see the case of $\gamma = 1$), the retrieving fidelity can be enhanced by optimizing the experimental noise factor σ for the MSO-based method. However, when the minimum normalized singular value associated with the most inefficient energy transport channel is larger than the experimental noise level ($\gamma \geq 81$), the achieved fidelity of the MSO-based method cannot surpass the result when the experimental noise factor σ is set to be 0, as can be seen in Fig. 3 (see also Fig. S2 of the Supplementary Material). When γ is further increased, T^{-1} is always the best reconstruction operator because it does not introduce new reconstruction noise. This means that although the MSO-based method can reduce the influence of experimental noise on information retrieval, the achieved fidelity has an upper limit imposed by its statistical nature, as shown by the cases of $\gamma = 81$ and $\gamma = 256$ in Fig. 3. Based on the results shown in Figs. 2 and 3, the demonstrated method is better than the state-of-the-art MSO-based method[10]. It should be pointed out that the achieved fidelity of this deterministic method can even outperform the deep learning methods demonstrated very recently[33].

We further demonstrate the optical information transmission for more complex wavefronts through two typical scattering media. The corresponding results for an MMF and a ground glass are shown in Figs. 4(a) and 4(b), respectively. Here,

Fig. 4. Near-unity fidelity retrieval of 256-level grayscale phase-encoded images of human faces and natural scene images through (a) an MMF and (b) a ground glass, respectively. The ground truths, the corresponding distributions of the output speckle, and the retrieved images are provided. The resolution of all transmitted and retrieved images is 32×32. These images are adapted from the CelebA dataset[40] and the ImageNet dataset[41], respectively.

256-level grayscale images of human faces and natural scenes adapted from the CelebA dataset[40] and ImageNet dataset[41] are used as the encoded phase wavefronts, respectively. As can be seen from Fig. 4, the maximal PCC/SSIM achieved in the experiment are up to 0.99/0.95, demonstrating the ability of delivering multilevel digital information through different scattering media. Similar images at the fourth and eighth columns of Figs. 4(a) and 4(b) indicate that the performance of the ground glass case is slightly better than that of the MMF case because of better experimental stability. These experimental results indicate that the phase information encoded in two spatial dimensions can be harnessed for transmitting information in parallel, facilitating the development of optical communication through strongly scattering media[42–44].

More importantly, the proposed method can also achieve light field information transmission through a scattering medium. The corresponding results for the MMF case are shown in Fig. 5. Here, fashion images adapted from the Fashion-MNIST dataset are used[45]. Both amplitude and phase information encoded in the wavefront can be retrieved with high fidelity using the ITM method, as shown by the results in the second and fifth rows of Fig. 5. The averaged PCC/SSIM of the retrieval phase (amplitude) based on the ITM method is 0.99/0.62 (0.97/0.61). Although the SSM method can also recover the light field information, it is essentially an approximate method[13]. Therefore, the experimentally achieved fidelity based on the SSM method is quite limited. For comparison, the retrieval results using the SSM method under the same experimental conditions are also provided in Fig. 5. As can be seen from these figures, the results of the ITM method are much better than that of the SSM method, where the corresponding PCC/SSIM of the retrieval phase (amplitude) based on the SSM method is only 0.84/0.39 (0.83/0.35). The high fidelity of light field information transmission through a scattering medium using only a single output light field E_{out} substantially increases the capacity of the optical information delivered over the MMF. It should be mentioned that the full-field retrieval results are not as good as the phase-only case because of the nonuniform amplitude distribution. The results over a ground glass are similar to the MMF case (see Fig. S3 of the Supplementary Material). All these results validate the superiority of our method for overcoming multiple scattering in scattering media and exploring light's multidimensions for delivering optical information.

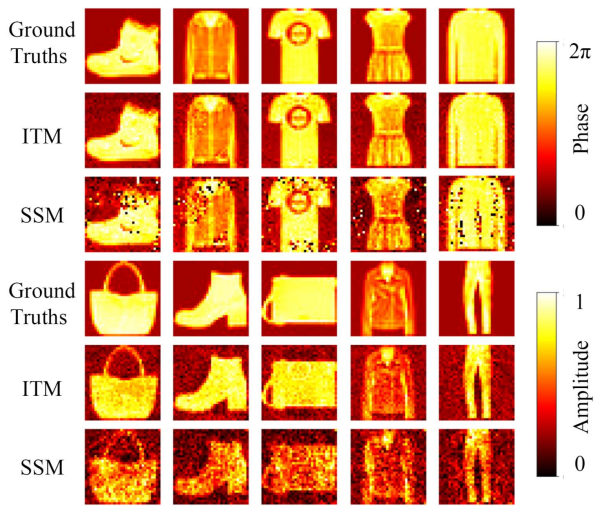

Fig. 5. Comparison of the complex light field imaging between the ITM and state-of-the-art SSM methods through an MMF. The first and fourth rows show the ground truths of the input phase and amplitude information, respectively. The second and fifth rows provide the complex light field reconstruction results based on the ITM method. The third and sixth rows show the complex light field reconstruction results based on the SSM method without post-optimization. The averaged PCC/SSIM of the retrieval phase (amplitude) based on the ITM method is 0.99/0.62 (0.97/0.61), while the averaged PCC/SSIM of the retrieval phase (amplitude) based on the SSM method is 0.84/0.39 (0.83/0.35). The resolution of all transmitted and retrieved images is 32 × 32. These images are adapted from the Fashion-MNIST dataset[45].

4. Conclusion

In conclusion, we revisit the problem of light field information transmission through scattering media using the ITM method, where the near-unity fidelity of the light field information transmission is experimentally demonstrated. Our method does not require any ensemble average and theoretical approximation. The achieved high fidelity of multiplexed data transmission suggests a better solution in addition to the state-of-the-art MSO-based method, the SSM method, and the deep learning method. Our results might facilitate the advanced developments for fiber communications and optical encryption. This technology can also be generalized to other multiple input and multiple output physical systems, including, but not limit to, acoustics[46] and wireless communications[47].

Acknowledgement

The authors acknowledge the inspired suggestions from Prof. Ziyang Chen and Mr. Weiru Fan of Huaqiao University. This work was supported by the National Key R&D Program of China (No. 2018YFB1801001), the National Natural Science Foundation of China (No. 62222505), and the Guangdong Introducing Innovative Entrepreneurial Teams of the Pearl River Talent Recruitment Program (Nos. 2019ZT08X340 and 2021ZT09X044).

References

1. H. Cao, A. P. Mosk, and S. Rotter, "Shaping the propagation of light in complex media," Nat. Phys. **18**, 994 (2022).
2. S. Yoon, M. Kim, M. Jang, Y. Choi, W. Choi, S. Kang, and W. Choi, "Deep optical imaging within complex scattering media," Nat. Rev. Phys. **2**, 141 (2020).
3. A. P. Mosk, A. Lagendijk, G. Lerosey, and M. Fink, "Controlling waves in space and time for imaging and focusing in complex media," Nat. Photonics **6**, 283 (2012).
4. J. Bertolotti and O. Katz, "Imaging in complex media," Nat. Phys. **18**, 1008 (2022).

5. M. Plöschner, T. Tyc, and T. Čižmár, "Seeing through chaos in multimode fibres," Nat. Photonics **9**, 529 (2015).
6. Z. Yu, H. Li, T. Zhong, J.-H. Park, S. Cheng, C. M. Woo, Q. Zhao, J. Yao, Y. Zhou, X. Huang, W. Pang, H. Yoon, Y. Shen, H. Liu, Y. Zheng, Y. Park, L. V. Wang, and P. Lai, "Wavefront shaping: a versatile tool to conquer multiple scattering in multidisciplinary fields," The Innov. **3**, 100292 (2022).
7. I. M. Vellekoop, A. Lagendijk, and A. P. Mosk, "Exploiting disorder for perfect focusing," Nat. Photonics **4**, 320 (2010).
8. P. Lai, L. Wang, J. W. Tay, and L. V. Wang, "Photoacoustically guided wavefront shaping for enhanced optical focusing in scattering media," Nat. Photonics **9**, 126 (2015).
9. G. Huang, D. Wu, J. Luo, L. Lu, F. Li, Y. Shen, and Z. Li, "Generalizing the Gerchberg–Saxton algorithm for retrieving complex optical transmission matrices," Photonics Res. **9**, 34 (2021).
10. S. Popoff, G. Lerosey, M. Fink, A. C. Boccara, and S. Gigan, "Image transmission through an opaque material," Nat. Commun. **1**, 81 (2010).
11. Y. Choi, C. Yoon, M. Kim, T. D. Yang, C. Fang-Yen, R. R. Dasari, K. J. Lee, and W. Choi, "Scanner-free and wide-field endoscopic imaging by using a single multimode optical fiber," Phys. Rev. Lett. **109**, 203901 (2012).
12. D. Loterie, S. Farahi, I. Papadopoulos, A. Goy, D. Psaltis, and C. Moser, "Digital confocal microscopy through a multimode fiber," Opt. Express **23**, 23845 (2015).
13. K. Lee and Y. Park, "Exploiting the speckle-correlation scattering matrix for a compact reference-free holographic image sensor," Nat. Commun. **7**, 13359 (2016).
14. Z. Cai, J. Chen, G. Pedrini, W. Osten, X. Liu, and X. Peng, "Lensless light-field imaging through diffuser encoding," Light. Sci. Appl. **9**, 143 (2020).
15. Z. Wen, Z. Dong, C. Pang, C. F. Kaminski, Q. Deng, J. Xu, L. Wang, S. Liu, J. Tang, W. Chen, X. Liu, and Q. Yang, "Single multimode fiber for *in vivo* light-field encoded nano-imaging," arXiv:2207.03096 (2022).
16. Z. Dong, Z. Wen, C. Pang, L. Wang, L. Wu, X. Liu, and Q. Yang, "A modulated sparse random matrix for high-resolution and high-speed 3D compressive imaging through a multimode fiber," Sci. Bull. **67**, 1224 (2022).
17. W. Li, B. Wang, T. Wu, F. Xu, and X. Shao, "Lensless imaging through thin scattering layers under broadband illumination," Photonics Res. **10**, 2471 (2022).
18. F. Wang, C. Wang, M. Chen, W. Gong, Y. Zhang, S. Han, and G. Situ, "Far-field super-resolution ghost imaging with a deep neural network constraint," Light. Sci. Appl. **11**, 1 (2022).
19. J. Oh, K. Lee, and Y. Park, "Single-shot reference-free holographic imaging using a liquid crystal geometric phase diffuser," Laser Photonics Rev. **16**, 2100559 (2022).
20. A. K. Singh, D. N. Naik, G. Pedrini, M. Takeda, and W. Osten, "Exploiting scattering media for exploring 3D objects," Light. Sci. Appl. **6**, e16219 (2017).
21. H. Yu, K. Lee, J. Park, and Y. Park, "Ultrahigh-definition dynamic 3D holographic display by active control of volume speckle fields," Nat. Photonics **11**, 186 (2017).
22. J. Park, K. Lee, and Y. Park, "Ultrathin wide-angle large-area digital 3D holographic display using a non-periodic photon sieve," Nat. Commun. **10**, 1304 (2019).
23. S. Li, C. Saunders, D. J. Lum, J. Murray-Bruce, V. K. Goyal, T. Čižmár, and D. B. Phillips, "Compressively sampling the optical transmission matrix of a multimode fibre," Light. Sci. Appl. **10**, 88 (2021).
24. X. Wei, J. C. Jing, Y. Shen, and L. V. Wang, "Harnessing a multi-dimensional fibre laser using genetic wavefront shaping," Light. Sci. Appl. **9**, 149 (2020).
25. L. Gong, Q. Zhao, H. Zhang, X.-Y. Hu, K. Huang, J.-M. Yang, and Y.-M. Li, "Optical orbital-angular-momentum-multiplexed data transmission under high scattering," Light. Sci. Appl. **8**, 27 (2019).
26. Q. Zhao, P.-P. Yu, Y.-F. Liu, Z.-Q. Wang, Y.-M. Li, and L. Gong, "Light field imaging through a single multimode fiber for OAM-multiplexed data transmission," Appl. Phys. Lett. **116**, 181101 (2020).
27. B. Pezeshki, F. Khoeini, A. Tselikov, R. Kalman, C. Danesh, and E. Afifi, "MicroLED array-based optical links using imaging fiber for chip-to-chip communications," in *Optical Fiber Communications Conference and Exhibition (OFC)* (2022), paper W1E.1.
28. S. Popoff, G. Lerosey, M. Fink, A. C. Boccara, and S. Gigan, "Controlling light through optical disordered media: transmission matrix approach," New J. Phys. **13**, 123021 (2011).
29. W. Fan, Z. Chen, V. V. Yakovlev, and J. Pu, "High-fidelity image reconstruction through multimode fiber via polarization-enhanced parametric speckle imaging," Laser Photonics Rev. **15**, 2000376 (2021).
30. P. Caramazza, O. Moran, R. Murray-Smith, and D. Faccio, "Transmission of natural scene images through a multimode fibre," Nat. Commun. **10**, 2029 (2019).
31. C. Zhu, E. A. Chan, Y. Wang, W. Peng, R. Guo, B. Zhang, C. Soci, and Y. Chong, "Image reconstruction through a multimode fiber with a simple neural network architecture," Sci. Rep. **11**, 896 (2021).
32. L. Wang, T. Qi, Z. Liu, Y. Meng, D. Li, P. Yan, M. Gong, and Q. Xiao, "Complex pattern transmission through multimode fiber under diverse light sources," APL Photonics **7**, 106104 (2022).
33. P. Tang, K. Zheng, W. Yuan, T. Pan, Y. Xu, S. Fu, Y. Wang, and Y. Qin, "Learning to transmit images through optical speckle of a multimode fiber with high fidelity," Appl. Phys. Lett. **121**, 081107 (2022).
34. S. M. Popoff, G. Lerosey, R. Carminati, M. Fink, A. C. Boccara, and S. Gigan, "Measuring the transmission matrix in optics: an approach to the study and control of light propagation in disordered media," Phys. Rev. Lett. **104**, 100601 (2010).
35. Y. Qi, C. Chang, and J. Xia, "Speckleless holographic display by complex modulation based on double-phase method," Opt. Express **24**, 30368 (2016).
36. O. Mendoza-Yero, G. Mínguez-Vega, and J. Lancis, "Encoding complex fields by using a phase-only optical element," Opt. Lett. **39**, 1740 (2014).
37. V. A. Marčenko and L. A. Pastur, "Distribution of eigenvalues for some sets of random matrices," Mat. Sb. **114**, 507 (1967).
38. R. Sprik, A. Tourin, J. de Rosny, and M. Fink, "Eigenvalue distributions of correlated multichannel transfer matrices in strongly scattering systems," Phys. Rev. B **78**, 012202 (2008).
39. C. W. Beenakker, "Random-matrix theory of quantum transport," Rev. Mod. Phys. **69**, 731 (1997).
40. Z. Liu, P. Luo, X. Wang, and X. Tang, "Deep learning face attributes in the wild," in *Proceedings of International Conference on Computer Vision (ICCV)* (2015), p. 3730.
41. O. Russakovsky, J. Deng, H. Su, J. Krause, S. Satheesh, S. Ma, Z. Huang, A. Karpathy, A. Khosla, M. Bernstein, A. C. Berg, and L. Fei-Fei, "ImageNet large scale visual recognition challenge," Int. J. Comput. Vis. **115**, 211 (2015).
42. D. J. Richardson, J. M. Fini, and L. E. Nelson, "Space-division multiplexing in optical fibres," Nat. Photonics **7**, 354 (2013).
43. R. G. H. van Uden, R. A. Correa, E. A. Lopez, F. Huijskens, C. Xia, G. Li, A. Schülzgen, H. de Waardt, A. M. J. Koonen, and C. M. Okonkwo, "Ultra-high-density spatial division multiplexing with a few-mode multicore fibre," Nat. Photonics **8**, 865 (2014).
44. A. E. Willner, Y. Ren, G. Xie, Y. Yan, L. Li, Z. Zhao, J. Wang, M. Tur, A. F. Molisch, and S. Ashrafi, "Recent advances in high-capacity free-space optical and radio-frequency communications using orbital angular momentum multiplexing," Philos. Trans. Royal Soc. A **375**, 20150439 (2017).
45. H. Xiao, K. Rasul, and R. Vollgraf, "Fashion-MNIST: a novel image dataset for benchmarking machine learning algorithms," arXiv:1708.07747 (2017).
46. A. Derode, P. Roux, and M. Fink, "Robust acoustic time reversal with high-order multiple scattering," Phys. Rev. Lett. **75**, 4206 (1995).
47. L. Zeng, D. C. O'Brien, H. Le Minh, G. E. Faulkner, K. Lee, D. Jung, Y. Oh, and E. T. Won, "High data rate multiple input multiple output (MIMO) optical wireless communications using white LED lighting," IEEE J. Sel. Areas Commun. **27**, 1654 (2009).